Journal of Computer-Aided Molecular Design (2005) 19: 329–340
DOI 10.1007/s10822-005-7003-0


# Dynamical aspects of TEM-1 β-Lactamase probed by molecular dynamics

Danilo Roccatano[a,d], Gianluca Sbardella[b], Massimiliano Aschi[a], Gianfranco Amicosante[c], Cecilia Bossa[b], Alfredo Di Nola[b] & Fernando Mazza[a,*]
[a]*Dipartimento di Chimica, Ingegneria Chimica e Materiali, Universitá degli Studi, V. Vetoio, 67010, L'Aquila, Italy;* [b]*Dipartimento di Chimica, Universitá degli Studi "La Sapienza", P.le A. Moro 5, 00185, Rome, Italy;* [c]*Dipartimento di Scienze e Tecnologie Biomediche, Universitá degli Studi, V. Vetoio, 67010, L'Aquila, Italy;* [d]*School of Engineering and Science, International University Bremen, Campus Ring, 1D-28725, Bremen, Germany*

Received 2 February 2005; accepted in revised form 9 May 2005


*Key words:* domain motion, H-bonding networks, Molecular Dynamics, Ω-loop, TEM-1 β-lactamase, water bridges

**Abstract**

The dynamical aspects of the fully hydrated TEM-1 β-lactamase have been determined by a 5 ns Molecular Dynamics simulation. Starting from the crystallographic coordinates, the protein shows a relaxation in water with an overall root mean square deviation from the crystal structure increasing up to 0.17 nm, within the first nanosecond. Then a plateau is reached and the molecule fluctuates around an equilibrium conformation. The results obtained in the first nanosecond are in agreement with those of a previous simulation (Diaz et al., J. Am. Chem. Soc., (2003) 125, 672–684). The successive equilibrium conformation in solution shows an increased mobility characterized by the following aspects. A flap-like translational motion anchores the Ω-loop to the body of the enzyme. A relevant part of the backbone dynamics implies a rotational motion of one domain relative to the other. The water molecules in the active site can exchange with different residence times. The H-bonding networks formed by the catalytic residues are frequently interrupted by water molecules that could favour proton transfer reactions. An additional simulation, where the aspartyl dyad D214–D233 was considered fully deprotonated, shows that the active site is destabilized.

*Abbreviations:* DynDom – dynamic domain; ED – essential dynamics; MD – Molecular Dynamics; RMSD – root mean square deviation; RMSF – root mean square fluctuation.

## Introduction

Class A serine β-lactamases represent the major source of bacterial resistance. These enzymes constitute a threat to human health since they can hydrolyze the β-lactam antibiotics according to the acylation-decylation pathway [1–5]. Therefore, they represent an important target for drug design [6, 7]. Although numerous crystallographic, spectroscopic, molecular mechanics and dynamics simulation, and site-directed mutagenesis studies have been performed (many references are reported in the review of Matagne et al. [3]), the catalytic mechanism and the exact role of the active site residues are still controversial and the relationship between variants and their catalytic properties are not yet completely understood [3, 8].

TEM-1 (Figure 1), the prototype of TEM family of class A β-lactamases, is formed by

*To whom correspondence should be addressed. Fax: +39-0862-433753; E-mail: mazza@univaq.it

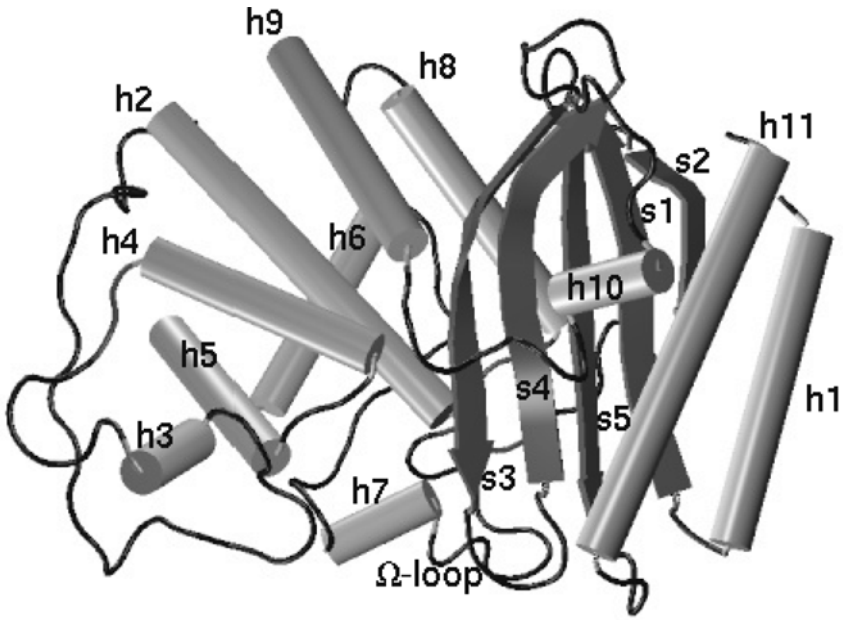


*Figure 1.* Cartoon representation of TEM-1 β-lactamase. The relevant structural elements are indicated.

two domains, an α/β and an all α domain [9]. The α/β domain includes a five-stranded antiparallel β-sheet onto which three helices (h1, h10 and h11) are packed. The α domain, composed by eight elices (h2–h9), is placed on the other side of the β-sheet. The two domains are connected by two hinge regions. Three salt bridges (E37–R61, R43–E64, R61–E64) and one H-bond (E37–V44) in the first hinge region, the salt bridge (R222–D233) and one H-bond involving the aspartyl dyad (D214–D233) in the second hinge region, prevent local structural modification to occur. The active site is in a groove between the two domains and it is surrounded by conserved elements bearing the five residues S70, K73, S130, E166, K234 more involved in the catalytic process. S70 and K73 are located at the beginning of h2 helix, S130 on the so-called invariant SDN loop forming one side of the catalytic cavity, E166 on the Ω loop forming the bottom edge of the active site and K234 on the innermost strand (s3) of the β-sheet forming the other side of the catalytic cavity.

A 1 ns Molecular Dynamics (MD) simulation of TEM-1 in aqueous solution was reported [10]. The moderate deviations and fluctuations obtained in this simulation, with particular regard to the Ω loop and the complex hydrogen bonding networks found in the active site, reproduce the situation found in the crystal structure of TEM-1[9].

It is known that proton transfer reactions largely depend on dynamical factors like the persistence of H-bonding network, the presence and residence time of water molecules and the mobility of residues. Since the dynamical behaviour of the free enzyme is a first step for the comprehension of the effects of the ligand binding in the active site, we have performed a 5 ns MD simulation of TEM-1 in aqueous solution. Starting from the crystallographic coordinates, the protein shows a relaxation in water with a Root Mean Square Deviation (RMSD) from the crystal structure increasing up to 0.17 nm, within the first nanosecond. Then a plateau is reached and the molecule fluctuates around an equilibrium conformation. The results obtained in the first nanosecond are in agreement with those of the previous simulation [10]. The successive equilibrium conformation of the protein in solution shows an increased overall mobility. A relevant part of the backbone dynamics implies a rotational motions of one domain relative to the other. Moreover a flap-like translational motion anchores the terminal part of the Ω loop to the body of the protein. Some H-bonds, both intramolecular and with water molecules, show a fluctuating behaviour.

Moreover, different residence times characterize the water molecules in the active site and the H-bonding networks of the catalytically relevant residues are frequently interrupted by water molecules, that could facilitate the proton transfer reactions. These represent new aspects that can not be observed in the first nanosecond of the simulation. Finally, the effect of the protonation state of the aspartyl dyad D214-D233 on the enzyme stability was probed by performing another MD simulation where the same aspartyl dyad was considered fully deprotonated.

## Methods

The starting model for simulations was taken from the crystal structure of TEM-1[9] (PDB code: 1BTL). The sulfate ion found in the active site was removed and replaced by water. The enzyme was solvated with water in a rectangular periodic box of $6.2\times7.8\times6.7$ nm. The water molecules making contacts smaller than 0.15 nm with protein atoms were removed. The total number of water molecules was $\approx 9000$. The simple point charge model [11] was used to describe the water molecules. Seven sodium counter-ions were added to neutralize the total box charge. Two different simulations, each of the same length (5 ns), considering the D214–D233 dyad in the mono and fully deprotonated state, respectively were performed. According to pKa calculations [12] the D214 was considered as the protonation site. However, similar results (data not reported) have been obtained in a 1 ns trial simulation considering the D233 as protonation site. In the simulations the temperature was maintained at 300 K by the isothermal coupling method [13]. The LINCS algorithm [14] was used to constrain all bond lengths. Rotational and translation motions of the protein were removed using the rototraslational constraint method [15]. A unitary dielectric permittivity was used. The calculation of the long range interactions was performed by the Particle Mesh Ewald method [16], using a grid spacing of 0.12 nm combined with a fourth-order B-spline interpolation to compute the potential and forces in between grid points. A non-bond pairlist cutoff of 0.9 nm was used and the pairlist was updated every four steps. All atoms were given an initial velocity obtained from a Maxwellian distribution at the desired initial temperature. After the minimization, the system was equilibrated by 100 ps of MD run with position restraints on the protein atoms. After the equilibration, the position restraints were removed and the system was gradually heated from 50 K to 300 K during 50 ps. All the MD runs and the analyses of trajectories were performed using the GROMACS software package [17].

To study the changes in backbone structure along the simulations, we have used the combined approach of the essential dynamics (ED) analysis and the dynamic domain (DynDom) identification method proposed by Hayward [18]. This combined approach has been successfully employed to analyze the dynamics of domains in different proteins [19, 20].

The Essential Dynamics analysis[21] allows the characterization of collective motions (essential motions) occurring during the MD simulation. The analysis was performed by building the covariance matrix of the positional fluctuations of the backbone atoms obtained from MD simulations. Upon diagonalization of the covariance matrix, a set of eigenvectors and their corresponding eigenvalues is generated defining a new set of generalized coordinates. The eigenvectors correspond to directions in a 3 N dimensional space (where N is the number of atoms used for the analysis) along which collective fluctuations of atoms occur. The eigenvalues represent the total mean square fluctuation of the system along the corresponding eigenvectors. By projecting the trajectory of the protein on the first two eigenvectors, the two configurations having the opposite largest displacement along the corresponding eigenvectors are extracted from each projections and used to perform the identification of the domain motion using the program DynDom [22].

## Results and Discussion

### *Deviations and fluctuations*

The time course of the backbone atoms RMSD of TEM-1 simulated in aqueous solution, relative to the crystal structure, is reported in Figure 2. The curve reaches a stationary value of 0.17 (s.d. 0.01) nm after 1 ns. It should be observed that the time spent in reaching the equilibration is significantly longer than that of the entire previous simulation ($\sim$1 ns) [10]. In order to identify the enzyme region

affected by major deviations, the RMSD of the backbone atoms of each residue, computed in the last 2 ns of the simulation, is reported in Figure 3 (top panel). The bordering regions of each domain present large deviations and the largest one affects the Ω loop region. The bottom panel of Figure 3 shows the Root Mean Squared Fluctuation (RMSF) of the backbone atoms of each residue computed in the last 2 ns. A comparison between the top and bottom panel of Figure 3 allows to deduce that the regions with large RMSD have low fluctuations. This indicates that the structural modifications of the enzyme, once in aqueous solution, are steady in time.

*Domain motion analysis*

The ED analysis of the simulated trajectory shows that, over a total of about 800 degrees of freedom, 80% of the overall motion is spread over the first 44 eigenvectors and the first two eigenvectors contribute for 50% of the overall fluctuations. The DynDom analysis reveals the presence of only one mechanical hinge axis that is described by the first eigenvector. This mechanical axis is displaced less than 0.4 nm from the $C^{\alpha}$ of residues 64, 185–187, 232, 246, 247 and 260, that belong to the hinge regions or are in their proximity. Consequently, the structural domains match the dynamical domains which are involved in a rotation amplitude of 12° around this axis, with 91% of closure motion. A colour representation of the enzyme regions (red and blue) involved by the rotational motion togheter with the hinge axis is given in Figure 4. The five-stranded β-sheet with helices h1 and h11 are the elements storing the elastic energy for the dynamical motion of the enzyme.

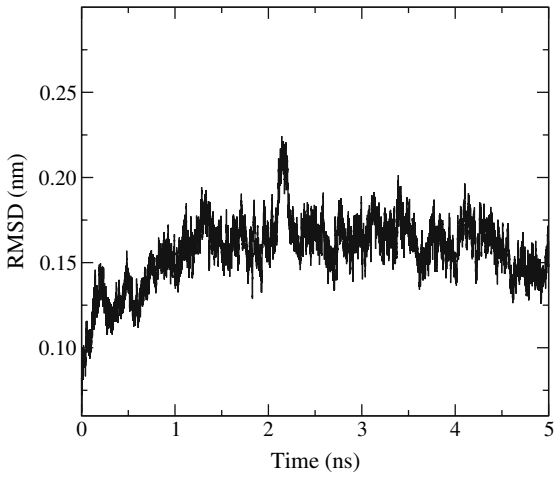


*Figure 2.* Time course of RMSD of the backbone atoms of TEM-1 in aqueous solution with respect to the crystal structure.

*Structure of the Ω loop in water*

The RMSD of the backbone atoms reported in Figure 3 reveal that the Ω loop region (161–179), forming one edge of the active site, is affected by large deviations and the P174 is the residue showing the largest deviation (> 0.45 nm). Moreover, this significant structural modification is concerted with the formation of a new H-bond between the N175 N of the Ω loop and the R65 CO of the body of the protein. As soon as this contact reaches H-bonding values (∼0.3 nm) the RMSD adopts an average steady value (∼0.2 nm). Both events take place simultaneously at the beginning of the simulation, evolve for about 500 ps and remain steady for the rest of the

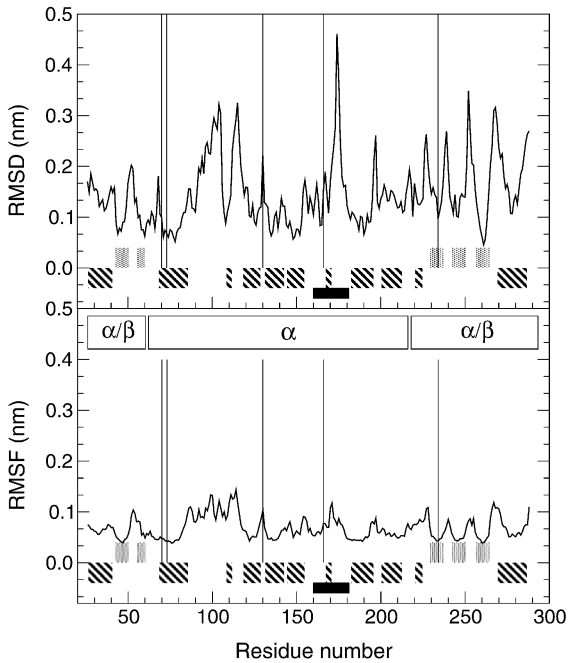


*Figure 3.* RMSD (top) and RMSF (bottom) of the backbone atoms for each residue of TEM-1 in aqueous solution along the last 2 ns of simulation. The vertical lines indicate the positions of the catalytic residues S70, K73, S130, E166, K234. The strands, helices and Ω loop regions are indicated by dotted, striped and full blocks. The α and α/β domains are also indicated.

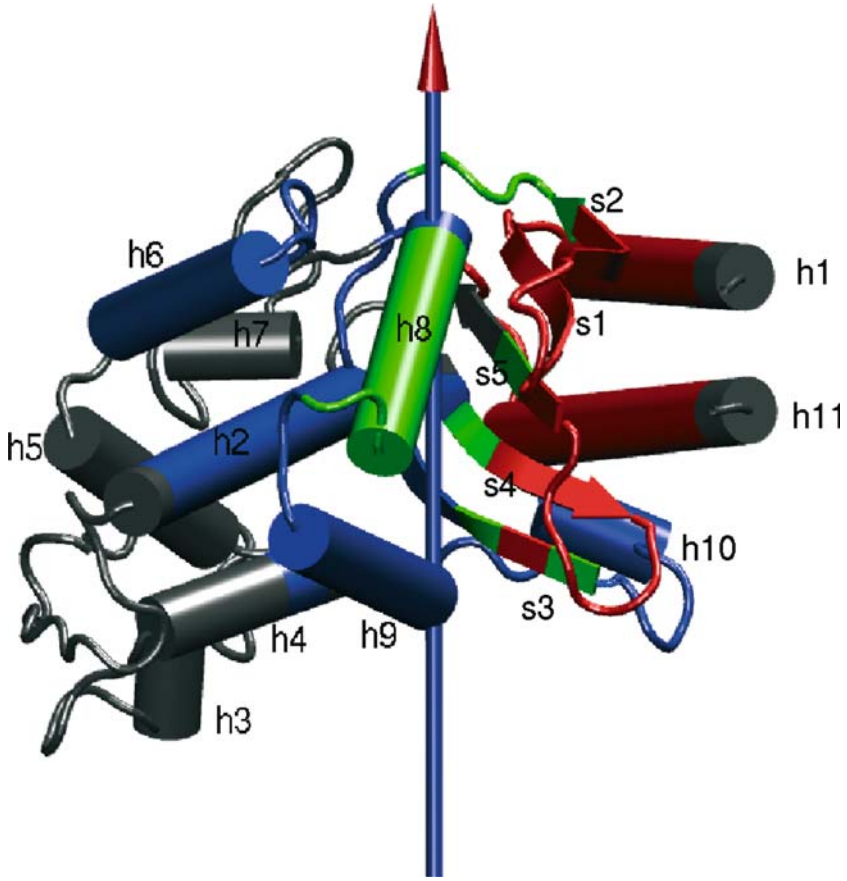


*Figure 4*. Representation of motion of the red regions relative to the blue ones occuring in the MD simulation. The arrow indicates the hinge axis, green the regions where the hinge bending takes place and black those regions not involved in the motion.

simulation. The positions adopted by the Ω loop relative to the body of the protein are presented in Figure 5 by the red and blue ropes standing for the initial (crystal) and final (water) situation, respectively. This flap-like translational motion, anchoring the Ω loop to the body of the protein, may be important for the enzyme activity, as it may help to prevent a complete hydration of the loop in aqueous solution, maintaining the catalytically important E166 in the vicinity of the active S70 residue. This motion of the Ω-loop is not reported in the previous simulation [10] and differs from the one observed in the MD simulation of the PC1 β-lactamase from *S aureus* [23]. In the last case a conformational transition of the Ω-loop is linked to the rupture of the important salt bridge $N^{\epsilon}$R164-$O^{\delta 2}$D179.

The following four salt bridges, $N^{\epsilon}$R164–$O^{\delta 2}$D179, $N^{\epsilon}$R178–$O^{\delta 2}$D176, $N^{\eta 1}$R164–$O^{\epsilon 1}$E171, $N^{\epsilon}$R161–$O^{\delta 1}$D163, found in the crystal structure of TEM-1 [9], confer polar character to the Ω-loop and are important for maintaining its conformation. Their time evolutions during the simulation were examined. The $N^{\epsilon}$R164–$O^{\delta 2}$D179 contact, linking the two ends of the loop, maintains an average steady value along the entire simulation. This salt bridge is an invariant among class A β-lactamases. The $N^{\epsilon}$R178–$O^{\delta 2}$D176 contact vanishes after about 500 ps and shows a fluctuating behaviour in the rest of the simulation. The contact $N^{\eta 1}$R164–$O^{\epsilon 1}$E171 becomes increasingly larger in the simulation. Finally, the $N^{\epsilon}$R161–$O^{\delta 1}$D163 salt bridge is lost after about 700 ps and, at about 2 ns of simulation, the $N^{\epsilon}$R161 engages OH158 in a new H-bond that is maintained for the rest of simulation.

Three H-bonds, OT181–NF66, NT181–OF66, NR161–OT180 were reported in the crystal structure of TEM-1 [9], as further stabilizing the N and C termini of the loop. The time evolutions of the

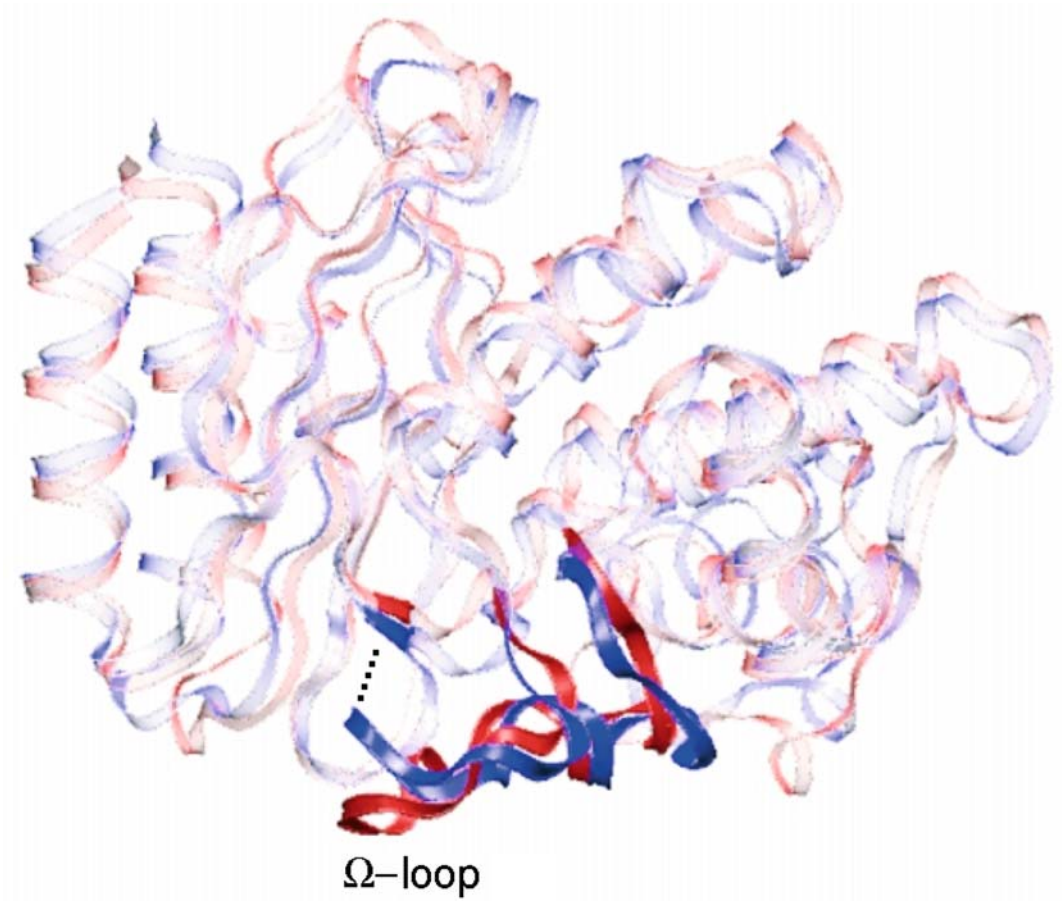


*Figure 5.* Flap-like translational motion of the Ω loop. The red and blue ropes represent the position adopted in the crystal and in solution, respectively. The dotted line indicates the N175-R65 H-bond formed in solution.

first two H-bonds show steady average values along the entire simulation, indicating stable H-bonding, while the maintainance of the third H-bond appears more perturbed along the trajectory.

*Water bridges in the active site*

The presence of water molecules H-bonded to active residues can be significant for the catalytic activity since it lowers the energy barrier in the proton transfer reactions involved in the acylation and deacylation of substrates. On the purpose we have examined the H-bonding networks formed by water molecules simultaneously engaging at least three H-bonds with the surrounding residues of the active site.

The time course of water bridged by D214, K234 and S235 residues is reported in Figure 6a. A water is simultaneously H-bonded with these residues for a time longer than 3 ns. Afterwards, it is immediately replaced by a new one forming the same network lasting until the end of the simulation. This stable presence of water is important since the catalytic K234 residue can have at disposal a slowly mobile water molecule. This network neatly corresponds to that found in the TEM-1 crystal [9].

The time course of water bridged by S70, E166 and N170 residues is reported in Figure 6b. The blank spaces there reported do not stand for water lack, but simply indicate absence of water simultaneously forming three H-bonds. Eleven different molecules exchange this position in the 5 ns simulation. The longest residence time is about 1 ns, indicating a water exchange faster than the previous case. The water bridging the S70 hydroxyl and E166 carboxylate groups has also been

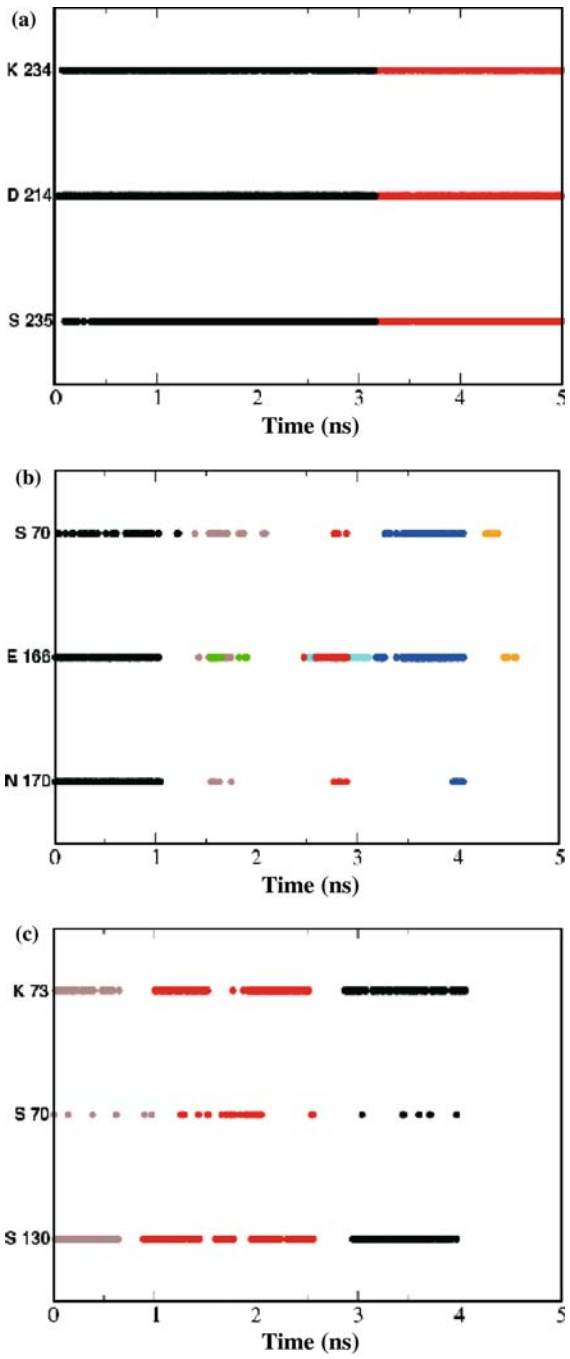


*Figure 6*. (a) Occurence of the water bridge with residues K234, D214 and S235; (b) Occurence of the water bridge with residues S70, K73, E166 and N170; (c) Occurence of the water bridge with residues K73, S70 and S130.

found in the TEM-1 crystal and in other class A β-lactamase crystal structures [9, 24–26]. It has been suggested that this conserved water may act as a relay in the reaction transfer of proton from S70 to E166 in the acylation step of the catalytic process. This proposal has been validated by recent findings. Electron Nuclear Double Resonance (ENDOR) spectroscopy revealed the presence of a water forming H-bonding with E166 in the acylenzyme of TEM-1 [27]. Further evidence emerges from the crystal structure of the adduct between a boronic acid inhibitor covalently linked to the $O^{\gamma}$S70 of the M182T TEM-1 mutant [28]. The interesting result emerging from this ultrahigh resolution structure is the protonated state of the E166 carboxylate group, indicating that a proton can be shuttled from S70 to E166 through the intermediate water. Even the MD simulation of TEM-1 [10] shows that the S70-W-E166 association is stable throughout the trajectory probed and the water does not exchange with the bulk. Our simulation not only confirms this result but, because of longer simulation times, it shows the possibility of water exchange. This is in better agreement with the functional role that the water should play at this site.

The active S70 is also involved, with the cooperation of the other two catalytic residues K73 and S130, in another network of H-bonds around water molecules differing from those previously examined. The time evolution is reported in Figure 6c. This alternative interaction of S70 might be considered in view of the still acylating capacity of the E166N TEM-1 mutant [29–31]. In this case the acylation should rely on an alternative mechanism without the direct participation of E166. One proposal assigns an active kinetic role to K73 and S130 residues that are strictly conserved in class A β-lactamases.

The presence of a water molecule in the "oxyanion hole" was also investigated. Several water molecules were found to bridge the residues S70 and A237 NH groups in the time period of the simulation, with a maximum residence time of 300 ps and a minimum below 50 ps.

### *H-bonding networks of catalytic residues*

The time course of the contact between $O^{\gamma}$S70 and $O^{\epsilon}$E166 is reported in Figure 7a. These residues practically never form direct H-bond along the simulated trajectory. Therefore, E166 cannot directly accept a proton from S70. This event can only be mediated by a water molecule assisting the nucleophilic attack of $O^{\gamma}$S70 on the substrate

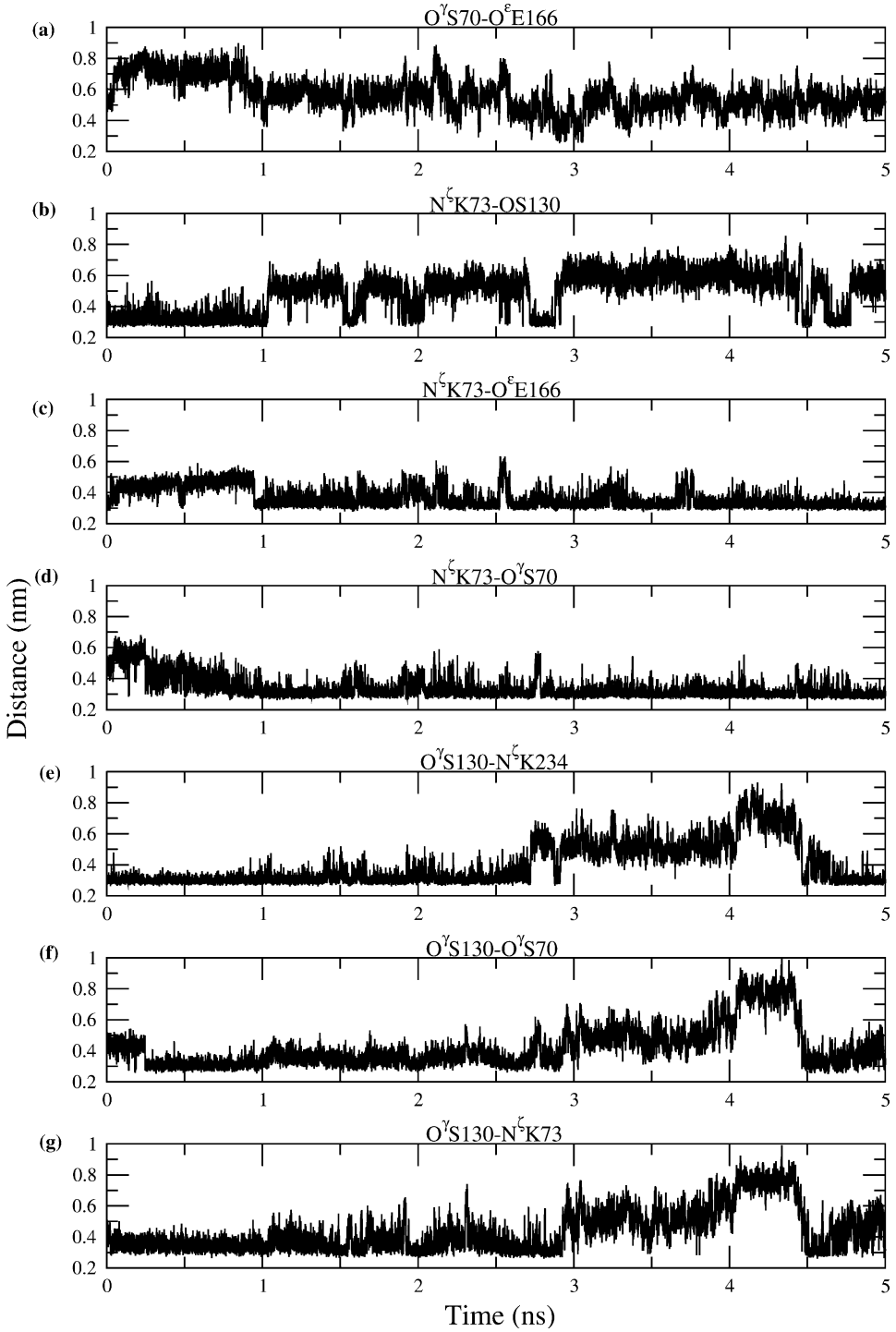


*Figure 7.* Time courses of the reported distances.

lactam carbonyl group, as discussed and shown in Figure 6b. This behaviour differs from that observed in the MD simulation of PC1 [23] where a short hydrogen bond (~2.8 Å) O$^{\gamma}$S70–O$^{\epsilon}$E166 forces the water away, indicating an S70-W-E166 unstable cluster.

The $N^{\zeta}$K73 and S130 carbonyl oxygen form direct H-bond only during the first nanosecond of simulation (Figure 7b). This is in accordance with the average value of 0.29 nm found for this contact in the 1 ns MD simulation [10]. However, our simulation shows that after 1 ns the direct H-bond is no longer maintained. In fact, this is competitive with the water bridging the same residues, as reported in Figure 6c.

The salt bridge $N^{\zeta}$K73–$O^{\epsilon}$E166 distance is longer during the first nanosecond of simulation and becomes shorter in the remaining part (Figure 7c). This interaction is competitive with the H-bond formation between the K73 ammonium and S130 CO groups (Figure 7b). As long as the two residues are engaged in H-bonding, the salt bridge is weaker, becoming stronger once the H-bond is no longer present. It has been proposed that an uncharged K73 might be obtained by the proton transfer K73 $\rightarrow$ E166 in the presence of substrate. In this way K73 could play the role of general base activating the $O^{\gamma}$S70 [32].

Even the H-bond $N^{\zeta}$K73-$O^{\gamma}$S70 (Figure 7d) is in competition with that between $N^{\zeta}$K73 and S130 carbonyl oxygen. The close proximity of the S70 and K73 side-chains, H-bonded even in the TEM-1 crystal [9], has suggested the alternative hypothesis of the likely involvement of K73 as the general base in the acylation reaction [3]. According to this hypothesis the K73 side-chain would act as the proton abstractor to increase the nucleophilicity of S70. However, the K73 terminal side-chain should be deprotonated to fulfil this task. On the other hand, it has also been observed that the positively charged alkylammonium group of K73 helps in orienting the S70 hydroxyl for efficient catalysis [3].

$O^{\gamma}$S130 forms direct H-bond with $N^{\zeta}$K234 (Figure 7e), $O^{\gamma}$S70 (Figure 7f) and $N^{\zeta}$K73 (Figure 7g), respectively. The almost simultaneous interruption of these interactions can be correlated to a water bridging K73 and S130 (Figure 6c). The interaction with K234 shows smaller fluctuations than those with the other two residues. Recently, it has been proposed that the acid catalyzed protonation of β-lactam N is favoured over the base catalyzed nucleophilic attack to the carbonyl carbon of lactam group [33]. According to this proposal, the N-protonation, initiating event of the catalytic reaction, would be catalyzed by a H-bonded cluster including the substrate carboxylate group, a water molecule and the couple of H-bonded S130 and K234 residues playing the role of proton donor. The direct H-bond S130–K234 interrupted by a water bridge, may well represent the preorganized aggregation in aqueous solution of free enzyme before substrate intervention.

An alternative pathway, for delivering the proton from S70 to the leaving β-lactam N in the acylation reaction, might be mediated by the substrate carboxylate with the following steps S70–S130-$COO^{-}_{substrate}$-$N_{substrate}$. This mechanism is similar to that of class C β-lactamases that is supported by the crystal structure of a complex formed by the S69G mutant of AmpC [34]. The $O^{\gamma}$S70–$O^{\gamma}$S130 direct H-bond (Figure 7f) may represent the step following the proton transfer from S130 to the substrate carboxylate.

Previous MD simulations [10] have shown that the polar cluster K73–E166 is linked to the $O^{\gamma}$S130–$N^{\zeta}$K234 H-bond through the OS130–$N^{\zeta}$K73 interaction. Our simulation shows that this link is lost after 1 ns, however it can be maintained through the other long lasting H-bond $O^{\gamma}$S130–$N^{\zeta}$K234.

### *Enzyme stability and protonation state of the D214–D233*

A key role in stabilizing the second hinge region of TEM-1 is played by D233. In fact, this residue simultaneously forms a salt bridge and a H-bond with R222 and D214, respectively. The contact $O^{\delta}$D214–$O^{\delta}$D233 of 0.28 nm, found in the crystal [9], indicates that one of the aspartates is likely protonated in the crystallization conditions (pH = 7.8). Arguments favouring D214 as being protonated have been reported [12]. Although it is generally agreed that only one of the aspartates is protonated for most of the time, the proton location likely changes during enzyme reaction [35, 36]. A search of the lowest contact between the carboxylate oxygens of D214 and D233 among the crystal structures of TEM family, at a resolution $< 0.2$ nm, reveals that the majority of these values fall in the range 0.24–0.31 nm. In few cases, always in presence of potassium ion, significantly larger values have been found, the largest one being 0.83 nm for TEM-32 (PDB code: 1L10). Surprisingly, this structure reveals that the potassium ion forms a salt bridge with $O^{\delta}$D233 (0.27 nm) shifting the $O^{\delta}$D214 to form a new short contact (0.27 nm)

with $N^{\eta}$R222. This indicates that the H-bonded aspartyl dyad can be easily destabilized.

We have also investigated the influence of protonation state of the D214–D233 dyad on the structural properties of TEM-1. On the purpose an additional MD simulation was performed for the enzyme with the fully deprotonated aspartyl dyad. The RMSD reaches a stationary value of 0.22 nm significantly larger than that obtained in the other simulation (Figure 2), thus indicating the effect caused by this proton removal. In order to give details on the residues and interactions involved in this structural modification, in Figure 8 we report the time course of three contacts monitored in the simulation of TEM-1 with the monopronated (black curve) and fully deproronated (grey curve) aspartyl dyad, respectively. The contact $O^{\delta}$D214–$O^{\delta}$D233 (Figure 8a) maintains a steady value indicating a stable H-bond (black curve) in agreement with the crystal structure, whereas it becomes increasingly larger (grey curve), because of repulsion between the negatively charged carboxylate oxygens. The salt bridge $N^{\eta}$R222–$O^{\delta}$D233 (Figure 8b) shows a stationary value of 0.34 nm (black curve) in accordance with the crystal, whereas values larger than 0.7 nm at the end of the simulation (grey curve) severely weaken this attractive interaction. The contact of 0.4 nm between $O^{\delta}$D214 and $N^{\zeta}$K234 formed after 2 ns (grey curve of Figure 8c) is indicative of a new salt bridge that cannot be present with the monoprotonated dyad (black curve) because of the protonated D214. Therefore, the fully deprotonated aspartyl dyad destabilizes the interactions connecting the second hinge region of TEM-1. In addition (data not shown) the deviations and fluctuations of the active site residues from the crystal structure, are larger than those obtained in the simulation of TEM-1 with the monoprotonated dyad. It is interesting to observe that the invariant D233, present in all class A β-lactamases, forms a salt bridge and a H-bond, both stabilizing the enzyme second hinge region. Consistently, it has been reported that replacement of D233 by other residues, strongly reduces the TEM-1 catalytic activity [37]. The H-bond $O^{\delta}$D214–$O^{\delta}$D233 and salt bridge $N^{\eta}$R222–$O^{\delta}$D233 connecting the second hinge region are destabilized both in D233 TEM-1 variants and in TEM-1 with the fully deprotonated aspartyl dyad.

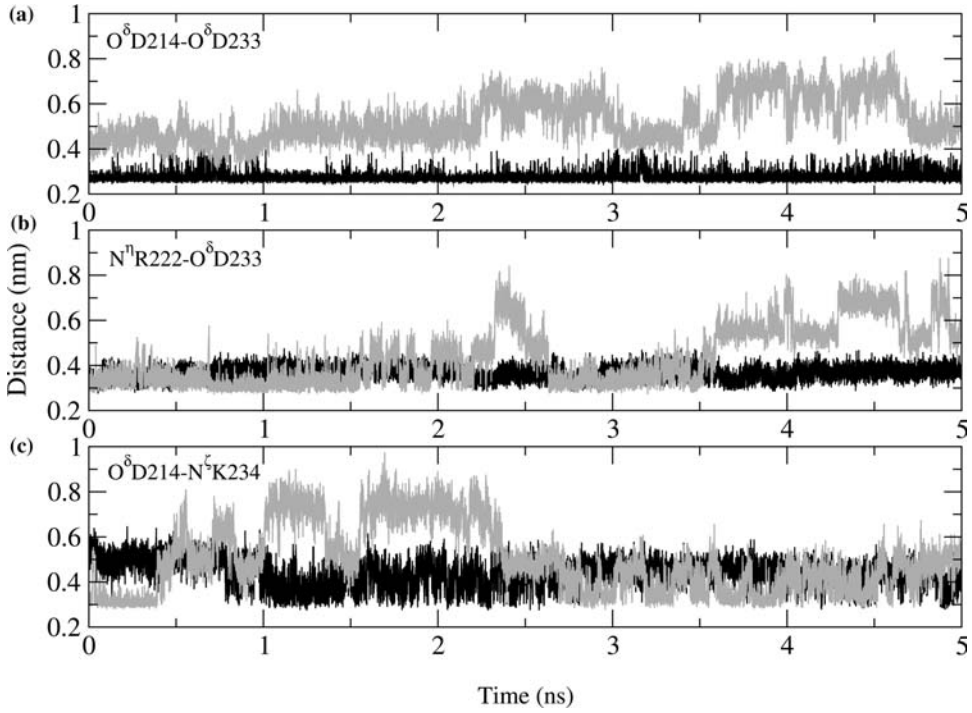


*Figure 8.* Time course of the indicated contacts monitored in the simulation of TEM-1 with the monopronated (black curve) and fully deproronated (grey curve) aspartyl dyad, respectively.

## Conclusions

A 5 ns trajectory of the TEM-1 β-lactamase in aqueous solution has been obtained by MD simulation. As shown in figure 2, the RMSD, with respect to the crystal structure, increases in the first nanosecond up to a plateau of 0.17 nm, then an equilibrium conformation is reached, that fluctuates around an average structure. The results obtained in the first non equilibrated part do not significantly differ from the ones previously reported by Diaz et al. [10]. Differently, in the equilibrated part of the simulation an increased mobility is observed. The dynamical behaviour is characterized by a closure motion around an axis passing near the two hinge regions. As a consequence the two structural domains pratically match the dynamical ones. The Ω loop, forming one edge of the catalytic region, undergoes a flap like translational motion anchoring its terminal part to the body of the protein through the new H-bond NN175–OR65. The water bridge S70-W-E166 is a long-lived interaction, and our simulation reveals that this conserved water can also exchange with the bulk on a ns time scale, emphasizing its functional role. Some H-bonds, both intramolecular and with water molecules, show a fluctuating behaviour. The complex H-bonding network found in the active site among the catalytically important residues, often interrupted by water molecules, can be relevant for the catalytic activity. Several preorganized H-bonded clusters proposed for different proton transfer reactions can be recognized. This great variety of possibilities can give reason that the route for acylation cannot be unique and alternative ways might be possible. The MD simulation of TEM-1 with the fully deprotonated aspartyl dyad D214–D233 shows that the R222–D233 salt bridge and the D214–D233 H-bond, important interactions connecting the second hinge region, are destabilized. A similar destabilization should occur in the practically inactive D233 TEM-1 variants. MD simulations of TEM-1 complexed with substrates are being currently performed.

## Acknowledgements

This work was supported by grant from MIUR (PRIN 2003 on Structure and dynamics of redox protein to A. D. N.). The authors thank Dr. S. Hayward, University of East Anglia, for useful discussions and support of DynDom program, Prof. S Mobashery, Univerity of Notre Dame, Indiana (U.S.A) for his criticism. CASPUR-Rome is acknowledged for computational facilities.

## References

1. Waley, S.G. Page, M.I. (Ed.), The Chemistry of β-lactams 1992, pp. 198–228, Chapman and Hall, Glasgow, U.K.
2. Galleni, M., Lamotte-Brasseur, J., Raquet, X., Dubus, A., Monnaie, D., Knox, J.R. and Frere, J.-M., Biochem. Pharmacol., 49 (1995) 1171.
3. Matagne, A., Lamotte-Brasseur, J. and Frere, J.-M., Biochem. J., 330 (1998) 581.
4. Wright, G.D., Chem. Biol., 7 (2000) 127.
5. Walsh, C., Nature, 406 (2000) 775.
6. Strynadka, N.C., Martin, R., Jensen, S.E., Gold, M. and Jones, J.B., Nat. Struct. Biol., 3 (1996) 688.
7. Ness, S., Martin, R., Kindler, A.M., Paetzel, M., Gold, M., Jensen, S.E., Jones, J.B. and Strynadka, N.C., Biochemistry, 39 (2000) 5312.
8. Yang, Y., Rasmussen, B.A. and Shlaes, D.M., Pharmacol. Therap., 83 (1999) 141.
9. Jelsch, C., Mourey, L., Masson, J.M. and Samama, J.-P., Proteins, 16 (1993) 364.
10. Diaz, N., Sordo, T.L., Merz, K.M. Jr. and Suarez, D., J. Am. Chem. Soc., 125 (2003) 672.
11. Berendsen, H.J.C., Grigera, J.R. and Straatsma, T.P., J. Phys. Chem., 91 (1987) 6269.
12. Swaren, P., Maveyraud, L., Guillet, V., Masson, J.-M., Mourey, L. and Samama, J.-P., Structure, 3 (1995) 603.
13. Allen, M.P. and Tildesly, D.J. Computer Simulation of Liquids. Oxford University Press, Oxford, 1987.
14. Hess, B., Bekker, H., Berendsen, H.J.C. and Fraaije, J.G.E.M., J. Comput. Chem., 18 (1997) 1463.
15. Amadei, A., Chillemi, G., Ceruso, M.A., Grottesi, A. and Di Nola, A., J. Chem. Phys., 112 (2000) 9.
16. Darden, T.A., York, D.M. and Pedersen, L.G., J. Chem. Phys., 98 (1993) 10089.
17. van der Spoel, D., van Drunen, R. and Berendsen, H.J.C., GROningen MAchine for Chemical Simulation, Department of Biophysical Chemistry, BIOSON Research Institute, Nijenborgh 4 NL-9717 AG Groningen, 1994.
18. Hayward, S. and Berendsen, H.J.C., Proteins, 30 (1998) 144.
19. deGroot, B.L., Hayward, S., vanAalten, D.M.F., Amadei, A. and Berendsen, H.J.C., Proteins, 31 (1998) 116.
20. Daidone, I., Roccatano, D. and Hayward, S., J. Mol. Biol., 339 (2004) 515.
21. Amadei, A., Linssen, A.B.M. and Berendsen, H.J.C., Proteins, 17 (1993) 412.
22. Hayward, S. and Lee, R.A., J. Mol. Graph. Model., 21 (2002) 181.
23. Vijayakumar, S., Ravishanker, G., Pratt, R.F. and Beveridge, D.L., J. Am. Chem. Soc., 117 (1995) 1722.
24. Knox, J.R. and Moews, P.C., J. Mol. Biol., 220 (1991) 435.
25. Lamotte-Brasseur, J., Dive, G., Dideberg, O., Charlier, P., Frere, J.M. and Ghuysen, J.M., Biochem. J., 279 (1991) 213.
26. Herzberg, O., J. Mol. Biol., 217 (1991) 701.

27. Mustafi, D., Sosa-Peinado, A. and Makinen, M.W., Biochemistry, 40 (2001) 2397.
28. Minasov, G., Wang, X. and Shoichet, B.K., J. Am. Chem Soc., 124 (2002) 5333.
29. Strynadka, N.C., Adachi, H., Jensen, S.E., Johns, K., Sielecki, A., Betzel, C., Sutoh, K. and James, M.N.G., Nature, 359 (1992) 700.
30. Guillaume, G., Vanhove, M., Lamotte-Brasseur, J., Ledent, P., Jamin, M., Joris, B. and Frere, J.-M., J. Biol. Chem., 272 (1997) 5438.
31. Massova, I. and Mobashery, S., Antimicrob. Agents Chemother., 42 (1998) 1.
32. Lietz, E.J., Truher, H., Kahn, D., Hokenson, M.J. and Fink, A.L., Biochemistry, 39 (2000) 4971.
33. Atanasov, B.P., Mustafi, D. and Makinen, M.W., Proc. Natl. Acad. Sci. U.S.A., 97 (2000) 3160.
34. Beadle, B.M., Trehan, I., Focia, P.J. and Shoichet, B.K., Structure, 10 (2002) 413.
35. Kashparov, I.V., Popov, M.E. and Popov, E.M., Adv. Exp. Med. Biol., 436 (1998) 115.
36. Torshin, I.Y., Harrison, R.W. and Weber, I.T., Protein Eng., 16 (2003) 201.
37. Denisov, V.P. and Halle, B., Faraday Discuss., 103 (1996) 227.